OPEN

Metabolic Choreography of Energy Substrates During DCD Heart Perfusion

Alessia Trimigno, PhD,[1] Jifang Zhao, PhD,[1] William A. Michaud, PhD,[2] Dane C. Paneitz, MD,[2] Chijioke Chukwudi, MD,[2] David A. D'Alessandro, MD,[2] Greg D. Lewis, MD,[2] Nathan F. Minie, MS,[2] Joseph P. Catricala, MS,[2] Douglas E. Vincent, BSME,[3] Manuela Lopera Higuita, PhD,[4] Maya Bolger-Chen, BsC,[4] Shannon N. Tessier, PhD,[4] Selena Li, MD,[2] Elizabeth M. O'Day, PhD,[1] Asishana A. Osho, MD,[2] and S. Alireza Rabi, MD, PhD[2]

Background. The number of patients waiting for heart transplant far exceeds the number of hearts available. Donation after circulatory death (DCD) combined with machine perfusion can increase the number of transplantable hearts by as much as 48%. Emerging studies also suggest machine perfusion could enable allograft "reconditioning" to optimize outcomes. However, a detailed understanding of the energetic substrates and metabolic changes during perfusion is lacking. **Methods.** Metabolites were analyzed using 1-dimensional ^{1}H and 2-dimensional ^{13}C-^{1}H heteronuclear spectrum quantum correlation nuclear magnetic resonance spectroscopy on serial perfusate samples (N = 98) from 32 DCD hearts that were successfully transplanted. Wilcoxon signed-rank and Kruskal-Wallis tests were used to test for significant differences in metabolite resonances during perfusion and network analysis was used to uncover altered metabolic pathways. **Results.** Metabolite differences were observed comparing baseline perfusate to samples from hearts at time points 1–2, 3–4, and 5–6 h of perfusion and all pairwise combinations. Among the most significant changes observed were a steady decrease in fatty acids and succinate and an increase in amino acids, especially alanine, glutamine, and glycine. This core set of metabolites was also altered in a DCD porcine model perfused with a nonblood-based perfusate. **Conclusions.** Temporal metabolic changes were identified during ex vivo perfusion of DCD hearts. Fatty acids, which are normally the predominant myocardial energy source, are rapidly depleted, while amino acids such as alanine, glutamine, and glycine increase. We also noted depletion of ketone, β-hydroxybutyric acid, which is known to have cardioprotective properties. Collectively, these results suggest a shift in energy substrates and provide a basis to design optimal preservation techniques during perfusion.

(*Transplantation Direct* 2024;10: e1704; doi: 10.1097/TXD.0000000000001704.)

Heart failure (HF) affects >6 million adults in the United States, threatening their health and well-being.[1] With an expected median survival of 12 y[2] and a significant improvement in quality of life,[3] heart transplant is the gold standard for the treatment of end-stage HF.[4] However, only about 4000 transplants were performed in the United States last year, with >3000 patients remaining on the waiting list.[5] Shortage of suitable hearts for transplant limits our ability to offer heart transplantation more broadly to patients with HF. To address this organ shortage, organs from extended-criteria donors and donation after circulatory death (DCD) are being used.

DCD has the potential to increase the number of transplantable organs by as much as 48%.[6] During DCD, the heart stops beating after withdrawal of life support. The "nonbeating" heart is then reanimated either in situ by placing the donor on cardiopulmonary bypass or by directly harvesting the heart and placing it on an ex vivo perfusion machine until transplant. The latter method, known as direct procurement

Received 14 June 2024.

Accepted 2 July 2024.

[1] Olaris, Inc., Framingham, MA.

[2] Division of Cardiac Surgery, Corrigan Minehan Heart Center, Massachusetts General Hospital, Corrigan Minehan Heart Center, Boston, MA.

[3] VentriFlo, Inc., Pelham, NH.

[4] Center for Engineering in Medicine and Surgery, Harvard Medical School and Massachusetts General Hospital, Shriner Children's Boston, Boston, MA.

This work was funded by Olaris, Inc.

A.T., J.Z., and E.M.O. are employees of Olaris, Inc and have ownership and salary interest in the company. The other authors declare no conflicts of interest.

A.T. and J.Z. participated in research design, performance of the research, data analysis, and writing of the article. W.A.M., D.C.P., C.C., D.A.D., G.D.L., N.F.M., J.P.C., D.E.V., M.L.H., M.S.J.B.-C., S.N.T., and S.L. participated in performance of the research and procurement of samples and clinical data. E.M.O. participated in research design, data analysis, and writing of the article. A.A.O. and S.A.R. participated in research design and in writing of the article.

A.T., J.Z., E.M.O., A.A.O., and S.A.R. contributed equally to this study.

Supplemental digital content (SDC) is available for this article. Direct URL citations appear in the printed text, and links to the digital files are provided in the HTML text of this article on the journal's Web site (www.transplantationdirect.com).

Correspondence: Elizabeth M. O'Day, PhD, 175 Crossing Blvd Suite 410, Framingham, MA 01702. (eoday@myolaris.com).

ISSN: 2373-8731

DOI: 10.1097/TXD.0000000000001704

and machine perfusion (MP), has been widely used for other organs, and the use of a commercially available system (TransMedics Organ Care System [OCS]) has been approved for heart transplant in the United States.[7] Recent data showed similar short- and intermediate-term survival of the recipients of hearts from DCD donors compared with traditional donation after brain death (DBD) heart recipients.[6,8,9] However, the rate of severe primary graft dysfunction (PGD), post-DCD transplantation is relatively high at ~15%,[10] leading to lower rates of DCD heart utilization at only 3.7%.[11] The underlying mechanism of PGD in DCD hearts is an area of active research. To reach its full potential further insights into DCD MP cellular processes are required.

The heart is highly metabolic and has a high demand for energy to support contraction.[12] A healthy heart exhibits metabolic plasticity and can use various substrates such as fatty acids (FAs), carbohydrates, amino acids, and ketones to meet this demand.[13] However, there is increasing evidence that in states of disease or stress the myocardium demonstrates increasing metabolic inflexibility.[14-17] Thus, ensuring adequate and appropriate energetic substrates are available during DCD MP is paramount to optimize outcomes.

The ideal perfusion composition and duration of perfusion remain undefined. In the OCS system, donor blood is mixed with proprietary solution of sugars, several amino acids, and electrolytes, but it does not include FAs or ketones. In a recent study, Truby et al[18] analyzed changes in a defined subset of energetic substrates including 66 acylcarnitines and 15 amino acids during DBD and DCD heart MP. They observed many fuel substrates were rapidly depleted, with specific patterns associated with DCD or DBD and that decreased levels of specific metabolites had increased odds of PGD.[18] Their results laid the foundation to question if the current perfusate cocktail is optimally providing the necessary nutrients for the heart during DCD MP.

In this study, we sought to expand upon these findings by examining a larger pool of metabolites using a global nuclear magnetic resonance (NMR) platform. Rather than targeted mass spectrometry approaches, which require a priori selection of metabolites or untargeted mass spectrometry, which faces technical challenges in terms of reproducibility, annotation, and data analysis,[19,20] we used a multidimensional global NMR platform that is highly reproducible and empowers identification and quantification of metabolites across a broad range of chemical classes and concentrations.[21] This enabled us to compare metabolite levels before and during perfusion and untangle the influence of several confounders that had not previously been explored. We hypothesized that energy substrates from donor blood would be used during perfusion and new energy substrates would be needed either through perfusate mixture or through metabolic processes within the heart. The results provide a basis to design new perfusate compositions and to test new strategies to preserve or improve heart quality during DCD MP.

MATERIALS AND METHODS

Patient Heart Perfusate Samples

The DCD direct procurement and perfusion process is detailed elsewhere.[22] After life support withdrawal, the donor is observed until circulation ceases. A 2–5 min waiting period is followed by sternotomy, draining 1-1. Five liters of donor blood into heparinized bags. This blood is mixed with priming solution to deair and prime the OCS pump. The heart is vented, aorta cross-clamped, and flushed with 1 L of 4 °C del Nido cardioplegia solution. The heart is then explanted, instrumented, and placed in the OCS machine for ex vivo perfusion at 34 °C. Coronary flow and left aortic pressures are monitored, with maintenance solution, epinephrine, and thyroid hormones added to the perfusate. Sampling ports collect perfusate samples. The baseline (BL) sample is collected pre-OCS placement or within 5 min after. The second sample is drawn 1–2 h postperfusion start. The last sample is collected precooling and flushing at the recipient operating room. **Figure S1** (**SDC**, http://links.lww.com/TXD/A694) illustrates the sample collection time points for each heart. Each sample, collected in 10 mL BD Vacutainer cell preparation tubes, undergoes centrifugation at 1500 relative centrifugal force for 15 min at room temperature. Subsequently, 3–4 mL of plasma is stored at –80 °C until thawed for metabolomic analysis.

Pig Heart Procurement

The pig heart was sourced from CBSET, Inc. (Lexington, MA), from a male Yorkshire swine, approximately 4 mo old, weighing 31 kg. Study approved by Massachusetts General Brigham Institutional Animcal Care and Use Committee. The pig was anesthetized and then euthanized with 2.7 g pentobarbital and 350 mg phenytoin sodium. After cessation of ventilatory support, a sternotomy was performed, the aorta was cannulated, the heart vented, and an aortic cross-clamp was placed. A 1 L flush of 4 °C del Nido solution arrested the heart via coronary circulation. Warm ischemia time totaled 15 min. Heart then cooled topically with ice, removed, and brought to laboratory for ex vivo perfusion. Cold ischemia time between cold flush and perfusion was 45 min, which is similar to the human heart preparation time for OCS.

Pig Heart Perfusate

Ex vivo circuit: The circuit (**Figure S2**, **SDC**, http://links.lww.com/TXD/A694) drains heart effluent into a reservoir via gravity through a cardiotomy chamber, where it is defoamed and filtered. A synchronized pulsatile pump (VentriFlo, Pelham, NH) driven by the heart's electrocardiogram signal pumps perfusate through an oxygenator (Terumo, Somerset, NJ) and compliance chamber mimicking arterial system compliance. Left atrium remains open. Drug infusion and sampling ports are included for accessibility. Priming: Circuit is primed with approximately 1.5 L of STEEN solution. Temperature maintained at 37 °C via integrated water heater and heat exchange unit. Monitoring: Aortic root pressure monitored via fluid-filled pressure transducer and recorded (LabScribe iWorX, Dover, NH). Aortic flow measured with ultrasonic flow probes (Transonic, Ithaca, NY). Electrocardiogram recorded with 3 electrodes. Perfusate collected from aorta and right atrium every 30 min. Heart weighed before and after run.

Analysis of Human Blood Hemolysis

Human blood obtained from hospital blood bank that were expired within 3–5 d and stored at 4 °C or deemed clinically unusable. One liter of blood circulated through a perfusion system with a roller pump (Sorin S5) and oxygenator (flow rates akin to OCS machine, ~1 L/min), minus a donor heart. Samples were collected hourly and processed same as the OCS samples.

NMR Sample Preparation

Proteins and macromolecules were removed, and metabolites were extracted via methanol/chloroform precipitation. The aqueous layer was partially evaporated under reduced pressure and lyophilized overnight. Lyophilized samples were dissolved in 0.21 mL of sodium phosphate buffer (pH 7.4) in deuterim oxide. A total of 10 mmol/L of deuterated sodium 2,2-dimethyl-2-silapentane-5-sulfonate (D, 98% dimethyl-2-silapentane-5- sulfonate-d6) was added to each sample for chemical shift referencing. A total of 180 µL of sample was then transferred to the NMR tube and analyzed.

NMR Data Collection and Processing

Metabolites were analyzed via 1-dimensional (1D) ^{1}H and 2-dimensional (2D) ^{13}C-^{1}H heteronuclear spectrum quantum correlation NMR spectroscopy collected on a Bruker AVANCE II solution-state 600 MHz spectrometer equipped with a liquid helium-cooled Prodigy TCI Cryoprobe (H/F, C, N), using a noesypr1d and hsqcetgpsisp2.2 pulse program and nonuniform sampling, respectively. One-dimensional spectra were processed on Topspin (Bruker Topspin 3.6.4; Bruker BioSpin, Rheinstetten, Germany), Matlab (Matlab R2015b; Mathworks, Inc., Natick, MA), and SigMa[23] (**Figure S3A, SDC**, http://links.lww.com/TXD/A694). The 1D data was used primarily for outlier detection, wherein all spectra were referenced to dimethyl-2-silapentane-5- sulfonate, normalized using probabilistic quotient normalization[24] and binned into 89 regions, corresponding to 31 metabolites, and 37 unknown signals. Principal component analysis of the 1D data showed that 1 BL sample (labeled 9082 from heart OCS1) was an outlier compared with all other samples (**Figure S3B, SDC**, http://links.lww.com/TXD/A694). This sample was, therefore, excluded from further analysis. The acquired nonuniform sampling 2D spectral data was processed and reconstructed using iterative soft thresholding, zero-filled, Fourier-transformed, and automatically phase-corrected to yield a final digital resolution of 2048 (N2) × 2048 (N1) points using the NMRPipe software package.[25] The processed 2D data was then used to generate peak lists using a total sum cutoff to prenormalize the data. Streaking from the primer and maintenance solution was still evident (**Figure S3C, SDC**, http://links.lww.com/TXD/A694), but these streaks were manually removed from each spectrum. Peaks were dynamically binned into clusters using Density-Based Spatial Clustering of Applications with Noise in both ^{1}H and ^{13}C dimensions.[26] Resonance clusters were median normalized and filtered using a zero-filter criterion of being present in at least 80% of all samples in 1 class. Chemical shift queries and metabolite annotations were performed using Olaris software.

Statistical Analysis

Because of nonnormal distribution of the data a Wilcoxon signed-rank test or Kruskal-Wallis (KW) nonparametric 1-way ANOVA on ranks was used to test for significant differences in measured NMR resonances between groups of interest based on the dependency of observations between time points. The test of significance was determined by a P value cutoff ($P < 0.05$) and adjusted based on false discovery rate (FDR) for multiple hypothesis testing correction. Fold change (FC) was calculated as the ratio of the median intensities of the 2 groups. An FC cutoff of 1.5 was used to determine significant changes, indicating that metabolites with FC >1.5 or <0.67 were considered upregulated or downregulated, respectively. All statistical analyses were performed using R 3.6.3 with ggplot2 for result visualization.[27]

GUIDELINES

Consent and Institutional Regulatory Process

This study was approved by the Massachusetts General Brigham Institutional Review Board (protocol number 2022P000405) and was declared exempt from requiring written consent. The study conforms to the Declaration of Helsinki guidelines.

RESULTS

Donor and Recipient Characteristics

Perfusate samples (N = 98) were collected from 32 DCD donor hearts transplanted into 33 recipients (Table 1). One donor heart was transplanted into a 45-y-old individual who had a devastating, nonrecoverable neurological insult because of a stroke 2 wk later. The family consented to transplantation, and this heart was then retransplanted (DCD transplant) into a 57-y-old individual after ex vivo perfusion on the OCS machine. To the best of our knowledge, this is the only reported DCD retransplant in the literature, and several differences were observed between the perfusion samples of the same heart including 8 metabolite resonances that were consistently and uniquely detected during the first perfusion across the 3 measured time points (**Figure S4** and **Table S1, SDC**, http://links.lww.com/TXD/A694).

Donor hearts averaged 32.7 y with 77.4% male, whereas recipients averaged 56.3 y with 74.2% male. Body mass index was not statistically different between donors and recipients (mean body mass index 29.2 versus 28.7). All donor hearts were successfully transplanted, but 9 suffered PGD, necessitating venoarterial extracorporeal membrane oxygenation within 24 h posttransplant. A forthcoming publication will detail metabolite signatures correlated with PGD.

Metabolite Changes From Baseline

The BL ^{1}H-^{13}C heteronuclear spectrum quantum correlation metabolite spectra were similar among hearts, suggesting a comparable starting composition; however, there were unique features associated with each heart (**Figure S5, SDC**, http://links.lww.com/TXD/A694), which could be attributable to donor-to-donor blood variability. To minimize individual differences, we used matched samples to perform a Wilcoxon signed-rank test comparing metabolite resonances at BL to those found in perfusate at 1–2, 3–4, or 5–6 h of perfusion (Figure 1A–C).

TABLE 1.

Donor and recipient characteristics

Characteristic	Donors	Recipients
Number (n)	32[a]	33
Age, y, mean (SD)	32.7 (10.0)	56.3 (10.9)
% Male	77.4%	74.2%
BMI, mean (SD)	29.2 (6.4)	28.7 (4.6)

Values are shown as mean ± SD where indicated.
[a]One heart was transplanted into 2 recipients (1 recipient died posttransplant and the heart was retransplanted).
BMI, body mass index.

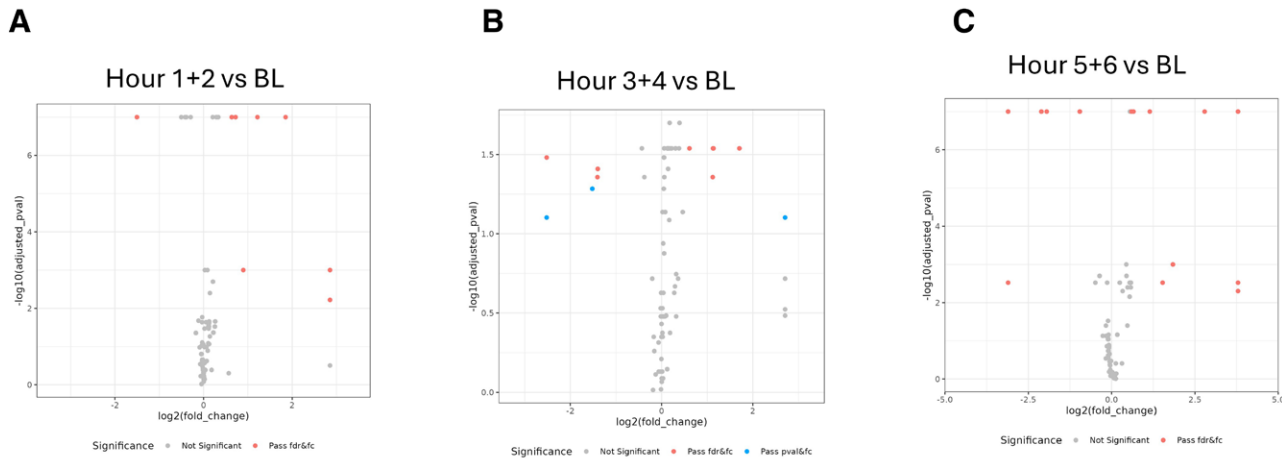

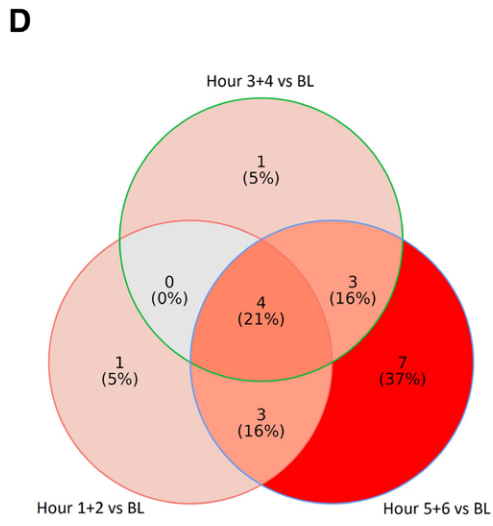

E

Comparison	Feature
Hour 1+2 vs BL & Hour 5+6 vs BL	X148, X324, X297
Hour 3+4 vs BL & Hour 5+6 vs BL	X151, X193, X157
Hour 1+2 vs BL & Hour 3+4 vs BL & Hour 5+6 vs BL	X360, X227, X188, X141
Hour 1+2 vs BL	X268
Hour 3+4 vs BL	X1628
Hour 5+6 vs BL	X173, X164, X150, X143, X338, X198, X35

FIGURE 1. Differential metabolite resonances from BL. Volcano plots highlighting significantly different metabolite resonances using Wilcoxon signed-rank test of significance with matched samples from BL to 1–2 h (A), 3–4 h (B), and 5–6 h (C). Resonances with absolute FC >1.5 and either a $P < 0.05$ (blue) or FDR-adjusted P value are (red) are highlighted. C and D, Comparison of the differential features from BL suggests several of the same resonances are altered from BL across perfusion. BL, baseline; FC, fold change; FDR, false discovery rate, PVAL, p-value.

We observed 8, 8, and 16 significantly different metabolite resonances (FDR-corrected P cutoff <0.05 and FC > 1.5) from BL at 1–2, 3–4, and 5–6 h, respectively. Features are given an XID number, for example, X188 based on the chemical shift. The altered resonances were highly overlapped, with 4 features consistently altered from BL (Figure 1D and E). At each time point, hierarchical clustering of the significant features showed near perfect separation from the BL samples to those on the perfusion machine (Figure 2A–C). Indeed, hierarchical clustering of the differential features from all matched BL analysis shows 3 main clusters, with nearly all the BL samples in 1 branch point, 1–2 h in another and more similar to BL, and the 3–4 or 5–6 h in the third (Figure 2D).

Metabolite Changes During Perfusion

To evaluate the changes during perfusion, using a matched Wilcoxon signed-rank test, we identified 5 significantly different (FDR-corrected P cutoff <0.05 FC >1.5) metabolite resonances between matched samples collected at 1–2 h and 3–4 h (N = 13) and 8 resonances between 1–2 and 5–6 h (N = 15) (Figure 3A and B). Because of lower sample size a KW test of significance was used to identify 3 significantly different (P cutoff <0.05 FC >1.5) metabolite resonances in non-matched samples between 3–4 h (N = 16) and 5–6 h (N = 13) (Figure 3C). Of note, these features did not meet the FDR-adjusted P value cutoff. Again, the altered resonances were highly overlapped, with 3 resonances constantly altered during perfusion, and all hits were previously identified as altered from BL (Figure 3D and E). Hierarchical clustering of the differential features had near perfect separation between 1–2 and 3–4 h or 1–2 and 5–6 h (Figure 4A and B). There was less separation between 3–4 and 5–6, which could be influenced by the small number of samples (Figure 4C). Clustering of all differential features had modest separation based on time (Figure 4D).

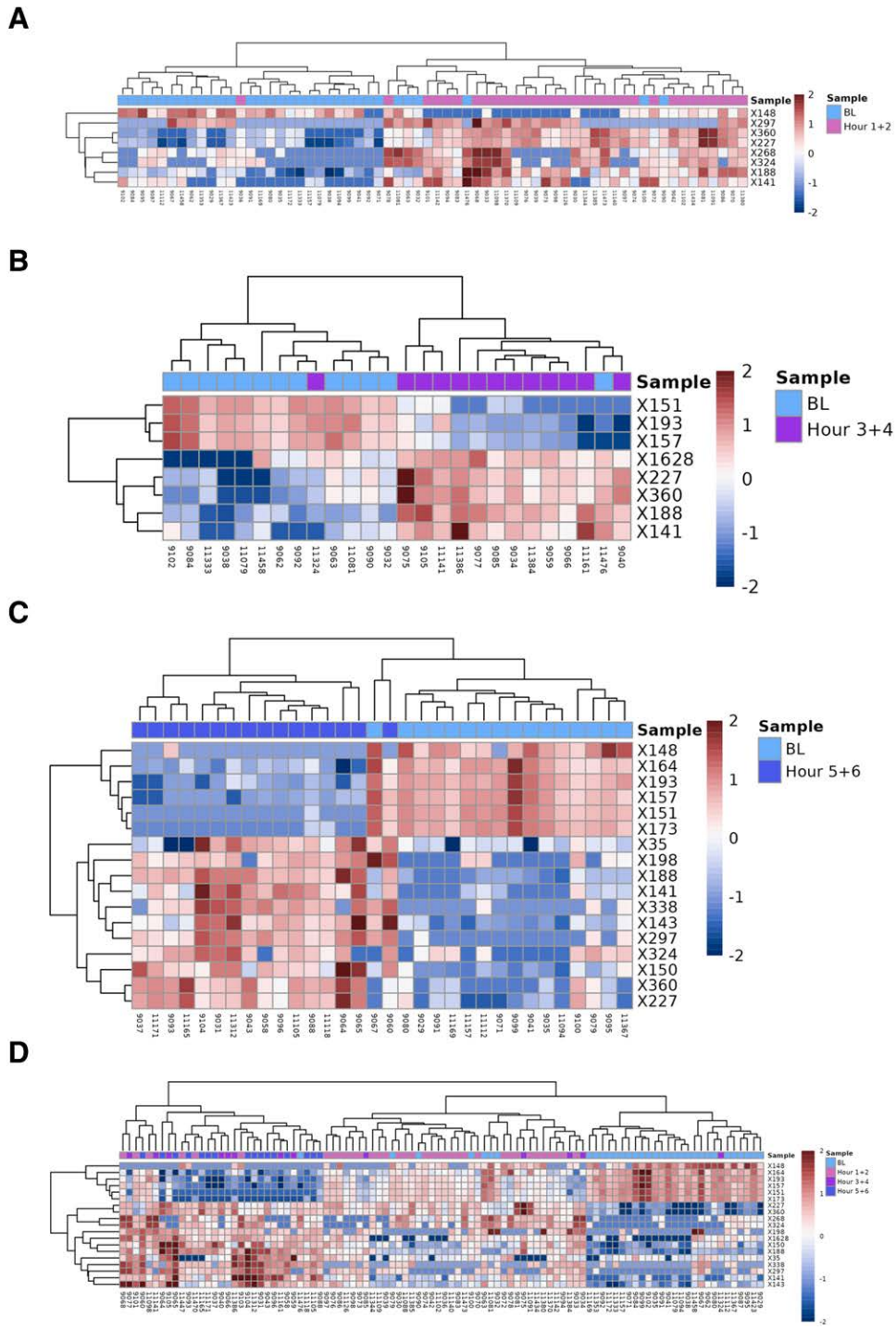

FIGURE 2. Heatmaps of differential metabolite resonances from BL. Hierarchical clusters of significantly different features (FDR $P < 0.05$ and absolute FC >1.5) from BL to 1–2 h (A), 3–4 h (B), and 5–6 h (C). The relative intensity of each resonance is color coded with red depicting a higher value and blue lower. Marked differences in metabolite resonances were observed from BL. Hierarchical clustering of all the differential features (D) suggest metabolite levels are altered based on time in perfusion. BL, baseline; FC, fold change; FDR, false discovery rate.

Annotation of Top Altered Metabolites During Perfusion

The top 18 altered features were annotated by comparing their chemical shifts to reference libraries of known metabolites and through spike-in experiments with standards (Table 2; **Figure S6, SDC**, http://links.lww.com/TXD/A694). Each resonance represents a unique carbon-hydrogen pair in a metabolite, and we were encouraged to see that many of the altered resonances indeed mapped to the same metabolite. We confirmed the following metabolites are significantly and consistently altered during perfusion: alanine (X188), creatine (X268 and X324), gluconic acid (X227 and X360), glutamine(X150), glycine (X141), hydroxyphenylacetic acid (X297 and X338), lysine (X143), phenylalanine (X1628 and x198), and succinate (X148). X35 did not match to any known metabolite in our library and, because it was in a region of the spectra that could

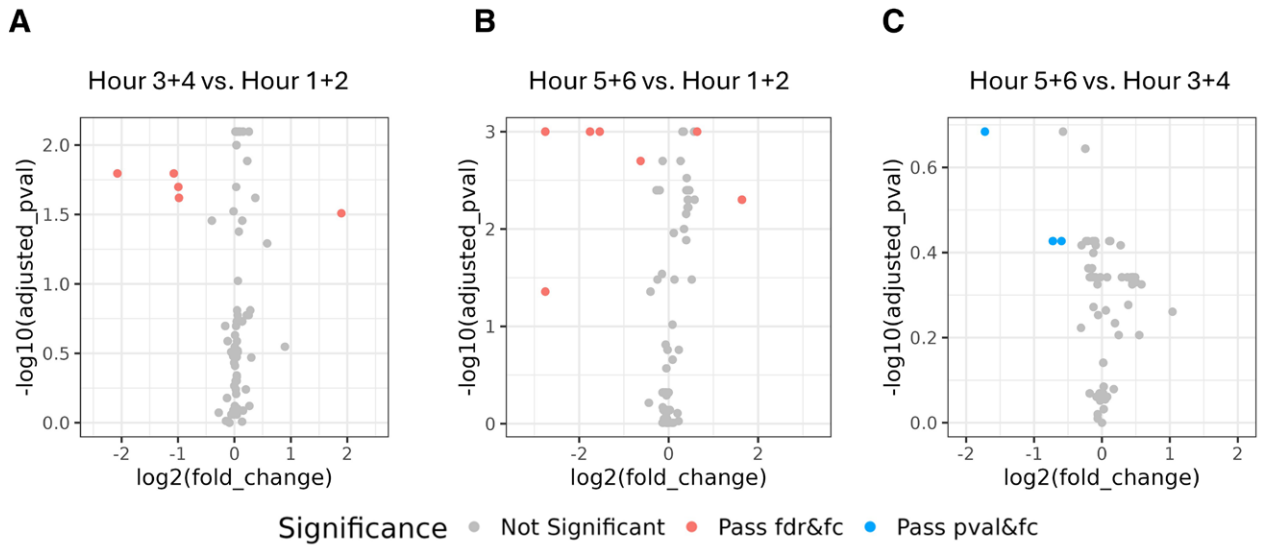

D

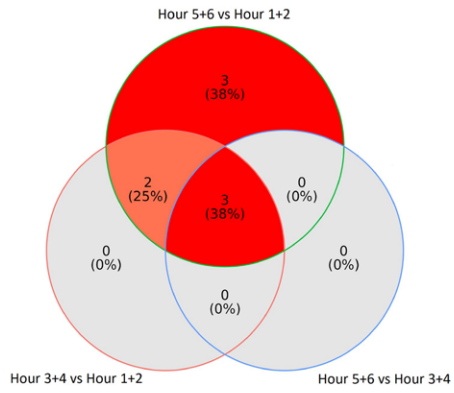

E

Comparison	Feature
Hour 5+6 vs Hour 1+2	X141, X164, X148
Hour 3+4 vs Hour 1+2 & Hour 5+6 vs Hour 1+2	X151, X338
Hour 3+4 vs Hour 1+2 & Hour 5+6 vs Hour 1+2 & Hour 5+6 vs Hour 3+4	X173, X157, X193

FIGURE 3. Differential metabolite resonances during perfusion. Volcano plots highlighting significantly different metabolite resonances using Wilcoxon signed-rank test of significance with matched samples from 1–2 to (A) 3–4 h and (B) 5–6 h and significant features using a Kruskal-Wallis (KW) test of significance from unmatched samples from 3–4 to 5–6 h (C). Resonances with absolute FC >1.5 and either a $P < 0.05$ (blue) or FDR-adjusted P value are (red) are highlighted. C and D, Comparison of the differential features suggests several of the same resonances are altered during perfusion. FC, fold change; FDR, false discovery rate, PVAL, p-value.

be influenced by the maintenance solution, we removed it from further analysis. Several of the metabolite resonances putatively matched to short-chain or medium-chain FAs. However, because of overlapping signals, we were unable to unambiguously determine the identities of these metabolite(s) and while efforts are underway for further structure elucidation, in the short term they were monitored by chemical shift/XID.

Role of Confounders

During perfusion, donor blood, priming solution, and maintenance solution (devoid of FAs but containing mannitol and various amino acids) circulate through the heart. We took a systematic approach to determine if the metabolic changes observed during MP were biased by these confounders (Figure 5A). For example, hemolysis occurs as red blood cells pass through the machine, indicated by characteristic color changes. To assess hemolysis's impact on the metabolic changes, recently expired human blood from the hospital blood bank circulated through a mock perfusion system mimicking OCS conditions. Serial samples collected >3 h showed only 5 of the top 18 resonances were detected with minimal change over time, indicating limited influence from hemolysis on our findings (Figure 5B).

To evaluate the contribution of the maintenance solution, we first extracted metabolites from an aliquot of the solution using the same protocol used for perfusate samples and then performed NMR. Of the top 18 resonances, 5 were detected in the maintenance solution (**Figure S7, SDC**, http://links.lww.com/TXD/A694). This was expected, as the composition of the maintenance solution is known (**Table S2, SDC**, http://links.lww.com/TXD/A694) and includes these amino acids. Thus, we cannot rule out that their increase during perfusion could be attributable to the addition of maintenance solution while the heart is on the machine.

To untangle the influence of the maintenance solution on the observed changes, we investigated altered features in a porcine model using STEEN, a blood-less, chemically defined medium in place of the maintenance solution (**Figure S2** and **Table S3, SDC**, http://links.lww.com/TXD/A694). From the pig heart perfusate samples, 12 top hits from human samples were detected. We observed a consistent decrease in FAs and an increase in alanine, creatinine, glutamine, and glycine, despite

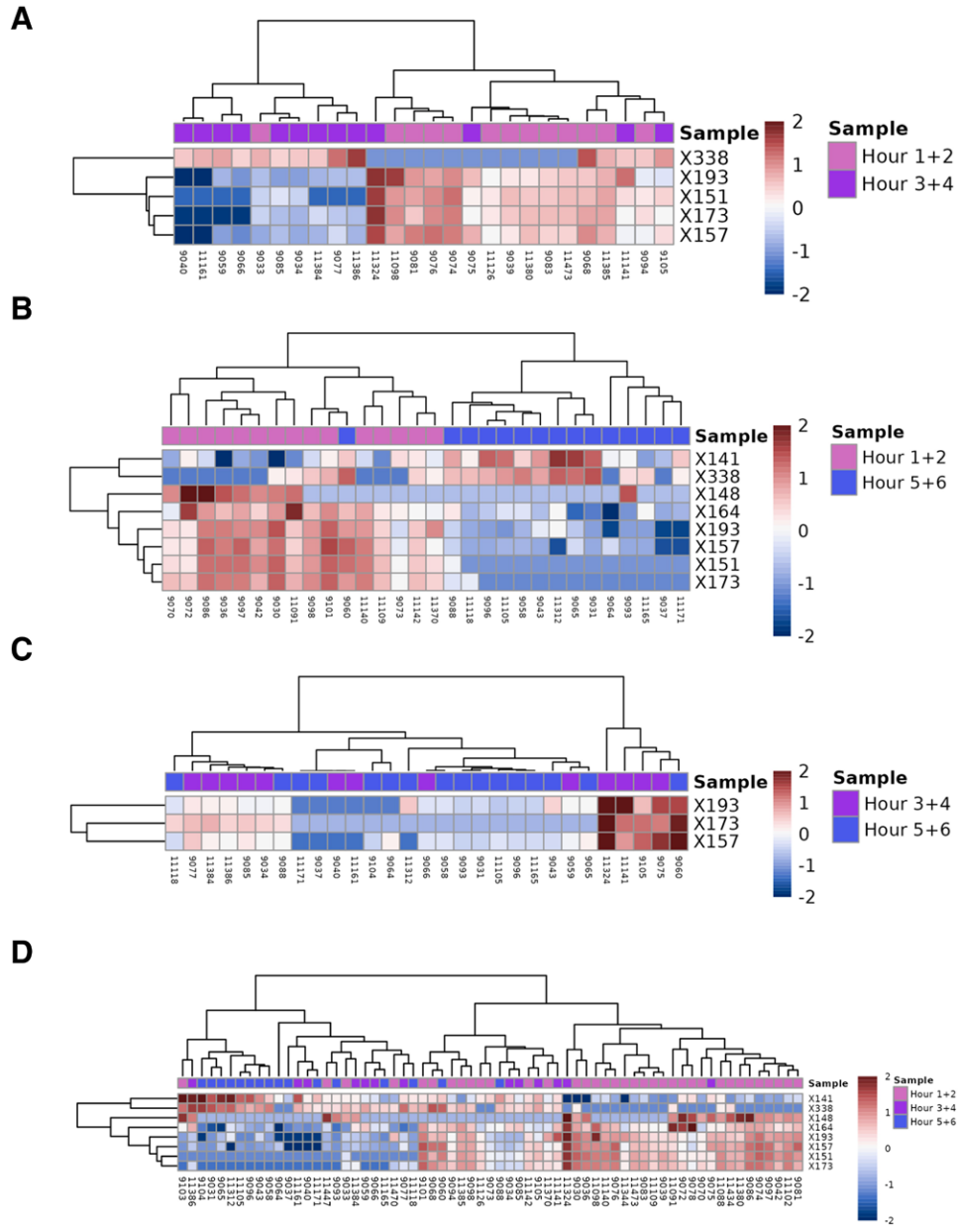

FIGURE 4. Heatmaps of differential metabolite resonances during perfusion. Hierarchical clusters of significantly different features (FDR $P <$ 0.05 and absolute FC >1.5) from 1–2 to (A) 3–4 h and (B) 5–6 h and clustering of significantly different resonances ($P < 0.05$ and absolute FC >1.5) from 3–4 to 5–6 h (C) and of all the differential features (D). FC, fold change; FDR, false discovery rate.

the absence of these constituents in STEEN (Figure 5C). These findings suggest that changes in FAs and amino acids are because of biological processes in the heart during perfusion, rather than confounders from hemolysis or OCS components.

Metabolic Pathway Analysis

Network analysis has the potential to reveal connections between metabolites and highlight metabolic pathways that may be altered during perfusion. We created a network with metabolite resonances depicted as nodes with the color representing the *P* value, size indicating the FC and shape indicating the directionality when comparing hours 5–6 to BL (Figure 6). Nodes were then connected through 3 possible edges: (1) correlation (orange), calculated from metabolite intensity across samples, and/or (2) structural similarity, with the Tanimoto coefficient as the similarity measure (blue), and/or (3) shared metabolic pathway (green), based on the Kyoto Encyclopedia of Genes and Genomes pathway database. From the network, it is clear these metabolites are connected through biological pathways (green lines) primarily related to amino acid metabolism; they are also correlated (orange lines), and several of the amino acids share structural similarities (blue lines). Succinate is part of the tricarboxylic acid (TCA) cycle and is linked to the amino acids, wherein their catabolism can provide additional TCA intermediates to fuel oxidative phosphorylation.

Metabolic Choreography of Energy Substrates During Perfusion

A healthy heart can use various substrates (FAs, glucose, lactate, ketones, and amino acids) to provide energy. We compared the levels of each of these substrates at BL to early, mid, and late perfusion (Figure 7). FAs were high at BL and then decreased

TABLE 2.

Top differential metabolite resonances during DCD perfusion

Feature	Hours 1 + 2 vs BL FC (*P* I FDR)	Hours 3 + 4 vs BL FC (*P* I FDR)	Hours 5 + 6 vs BL FC (*P* I FDR)	Hours 3 + 4 vs hours 1 + 2 FC (*P* I FDR)	Hours 5 + 6 vs hours 1 + 2 FC (*P* I FDR)	Hours 5 + 6 vs hours 3 + 4 FC (*P* I FDR)	Annotation	1H ppm	13C ppm
X188	1.556 (0 I 0)	2.184 (0.005 I 0.029)	2.215 (0 I 0)	1.292 (0.006 I 0.024)	1.482 (0 I 0.001)	1.088 (0.023 I 0.374)	Alanine	1.47	18.97
X268	1.650 (0 I 0)	Inf (0.103 I 0.192)	1.126 (0.038 I 0.069)	0.913 (0.541 I 0.664)	0.736 (0.402 I 0.61)	0.808 (0.449 I 0.599)	Creatine	3.92	56.54
X324	Inf (0 I 0.001)	Inf (0.221 I 0.328)	2.889 (0.001 I 0.003)	0.940 (1 I 1)	1.171 (0.093 I 0.174)	1.018 (0.659 I 0.823)	Creatine	3.03	39.75
X227	2.323 (0 I 0)	2.200 (0.002 I 0.029)	3.579 (0 I 0.001)	1.007 (0.273 I 0.389)	0.996 (0.934 I 0.978)	0.889 (0.254 I 0.455)	Gluconic acid	4.03	73.86
X360	3.614 (0 I 0)	3.263 (0.002 I 0.029)	Inf (0 I 0)	0.960 (0.191 I 0.309)	1.000 (0.277 I 0.477)	0.962 (0.405 I 0.558)	Gluconic acid	4.13	76.74
X150	1.259 (0 I 0)	1.314 (0 I 0.02)	1.515 (0 I 0)	1.113 (0.001 I 0.008)	1.261 (0 I 0.001)	1.040 (0.38 I 0.544)	Glutamine	2.44	33.65
X141	1.863 (0 I 0.001)	2.173 (0.017 I 0.044)	6.931 (0 I 0)	1.495 (0.017 I 0.051)	1.556 (0 I 0.001)	1.21 (0.096 I 0.383)	Glycine	3.55	44.34
X297	Inf (0.002 I 0.006)	Inf (0.037 I 0.079)	Inf (0 I 0)	1.230 (0.23 I 0.339)	1.323 (0 I 0.003)	1.078 (0.079 I 0.374)	Hydroxyphenylacetic acid	7.18	133.53
X338	ZF	1.378 (0.031 I 0.073)	Inf (0.001 I 0.003)	Inf (0.009 I 0.031)	Inf (0.002 I 0.005)	1.226 (0.254 I 0.455)	Hydroxyphenylacetic acid	6.88	118.67
X143	1.156 (0 I 0)	1.238 (0.008 I 0.029)	1.578 (0 I 0)	1.214 (0.057 I 0.155)	1.203 (0 I 0.002)	1.054 (0.254 I 0.455)	Lysine	3.01	41.82
X1628	1.194 (0.013 I 0.03)	1.525 (0.001 I 0.029)	1.465 (0 I 0)	1.194 (0 I 0.008)	1.240 (0 I 0.001)	0.991 (0.826 I 0.882)	Phenylalanine	7.34	132.15
X198	Inf (0.24 I 0.313)	Inf (0.197 I 0.3)	Inf (0.002 I 0.005)	1.163 (0.068 I 0.168)	1.268 (0.004 I 0.01)	1.128 (0.677 I 0.833)	Phenylalanine	7.42	131.82
X148	0 (0 I 0)	0 (0.038 I 0.079)	0 (0.001 I 0.003)	ZF	0 (0.021 I 0.044)	ZF	Succinic acid	2.34	36.33
X151	0.705 (0 I 0)	0 (0.01 I 0.033)	0 (0 I 0)	0 (0.003 I 0.016)	0 (0 I 0.001)	ZF	FA	1.27	33.76
X157	0.757 (0 I 0)	0.377 (0.017 I 0.044)	0.259 (0 I 0)	0.502 (0.005 I 0.02)	0.344 (0 I 0.001)	0.662 (0.025 I 0.374)	FA	1.28	31.18
X164	0.818 (0 I 0)	0.741 (0.006 I 0.029)	0.516 (0 I 0)	0.921 (0.127 I 0.258)	0.648 (0 I 0.002)	0.672 (0.005 I 0.207)	FA	1.55	28.42
X173	0.749 (0 I 0)	0.349 (0.021 I 0.052)	0 (0 I 0)	0.475 (0.003 I 0.016)	0 (0 I 0.001)	0 (0.005 I 0.207)	FA	1.27	24.66
X193	0.764 (0 I 0)	0.379 (0.013 I 0.039)	0.232 (0 I 0)	0.506 (0.006 I 0.024)	0.296 (0 I 0.001)	0.606 (0.038 I 0.374)	FA	0.85	16.16

The FC, *P* value, and FDR-adjusted *P* value is provided for each analysis. Features are highlighted in green if they passed a $P < 0.05$ and absolute FC > 1.5; yellow if they had a $P < 0.05$. Inf indicates a FC of infinity which occurs when the feature was missing or below the limit of detection in one set of samples. ZF indicates analysis where a feature did not pass our 80% zero-filter criteria.

BL, baseline; DCD, donation after circulatory death; FA, fatty acid; FC, fold change; FDR, false discovery rate; 1H ppm and 13C, chemical shift position of each carbon-hydrogen feature.

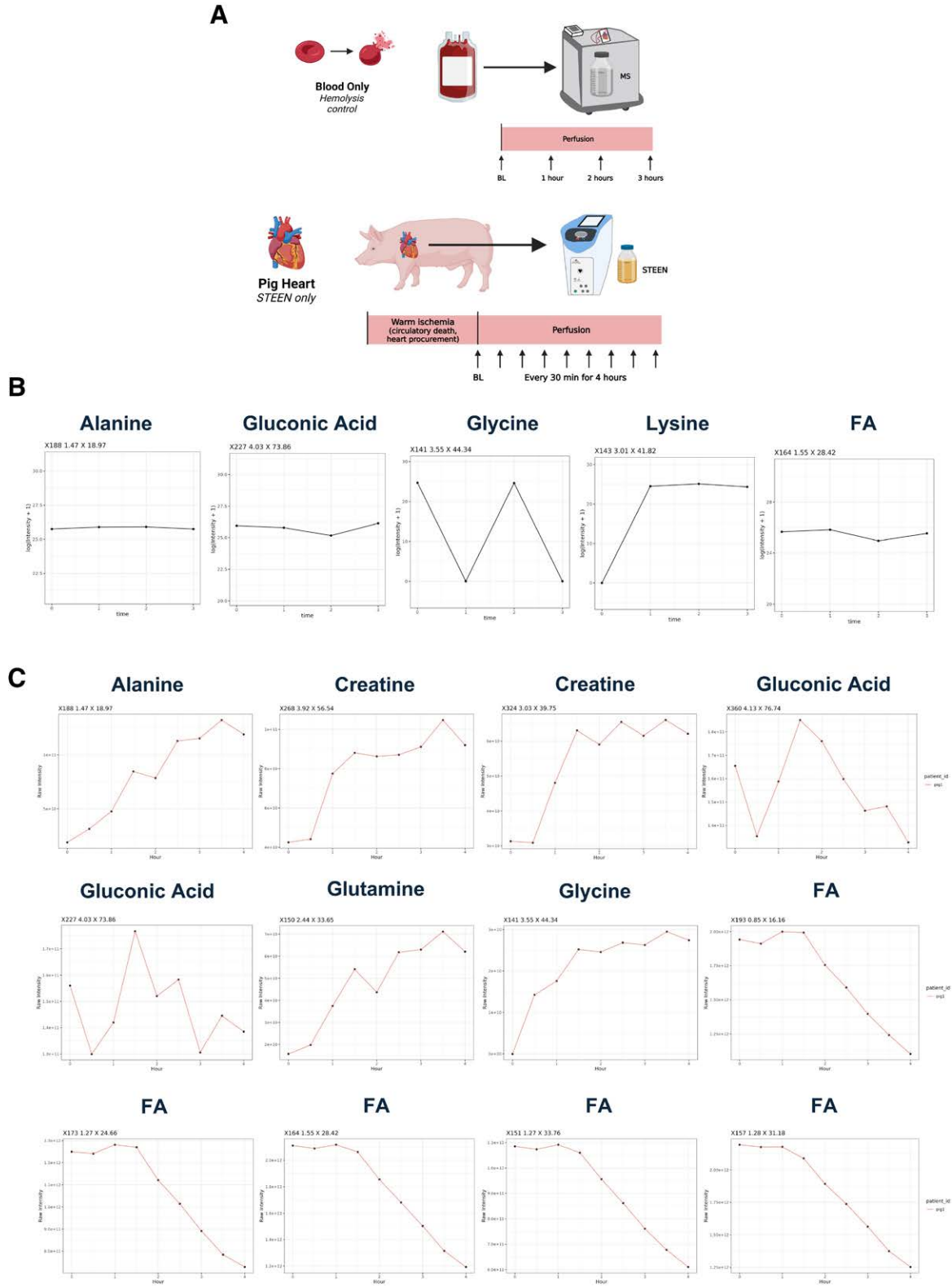

FIGURE 5. Role of confounders in metabolite measurements. A, Study design. For hemolysis control, blood alone was run through a mock perfusion machine, with samples taken every hour for 3 h of perfusion. For porcine control, a pig heart was perfused with STEEN solution and without maintenance solution or added blood. Samples were taken every 30 min for 4 h of perfusion. B, Metabolite resonance level change across time for the detected (5/18) top differential features in hemolysis control conditions. C, Metabolite resonance level change across time for the detected (12/18) top differential features detected in porcine model. Annotations are shown above resonance XID. BL, baseline; FA, fatty acid.

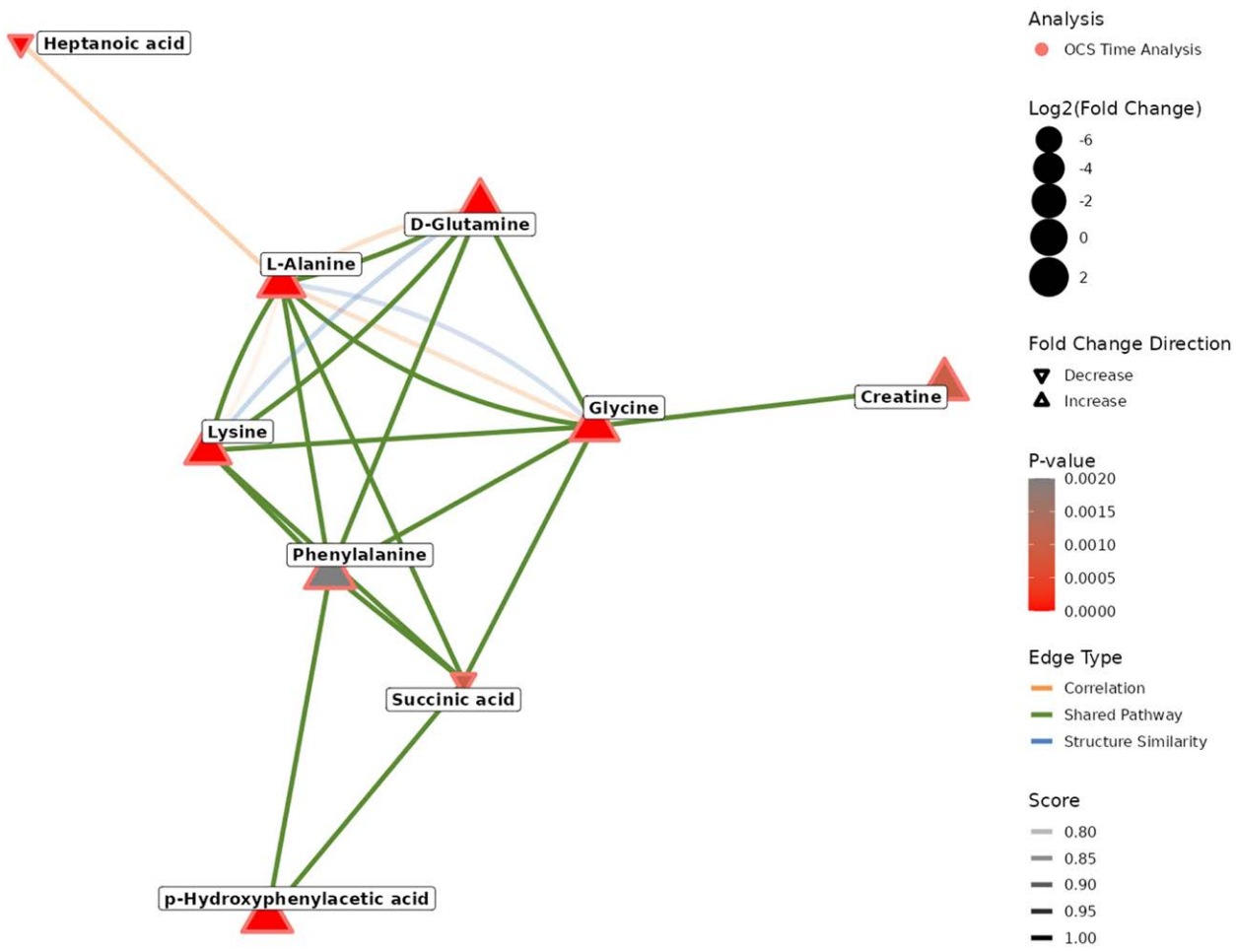

FIGURE 6. Network analysis of top altered metabolites. Network map using annotated metabolites as nodes (heptanoic acid was used as a representative FA). The size of node indicates the FC while direction of node indicates direction of FC from BL. Wilcoxon signed-rank test *P* value is depicted by color inside each node. Color of the edge line connecting nodes indicates the type of connection (orange, correlation, calculated from metabolite intensity across samples; green, biochemical pathway, based on KEGG database; and blue, structural similarity, with Tanimoto coefficient as similarity measure). Intensity of line indicates score of connection. For correlation and structural similarity, only connections with a score >0.75 are shown. BL, baseline; FA, fatty acid; FC, fold change; KEGG, Kyoto Encyclopedia of Genes and Genomes; OCS, TransMedics Organ Care System.

during MP. The ketone β-hydroxybutyric acid (β-OHB) showed a decreasing trend from BL to below our limit of detection after 4 h of perfusion. β-OHB was not included as a top hit as it was just beyond our 80% zero-filter criteria where it was present in only 78% samples at a single time point. Glucose increased from BL but remained consistent through later perfusion time points. The increase from BL is likely attributable to sugar present in Priming Solution. The core amino acids (alanine, glycine, and glutamine) that were observed in both human and porcine models increased from BL and from 1 time point to the next during MP. Lactate did not significantly change, which is expected as it is closely monitored, and the maintenance solution is adjusted to keep levels consistent. The inverse choreography, between FAs and amino acids suggest a shift in energetic substrate availability during DCD MP.

DISCUSSION

The heart is referred to as "omnivorous" meaning it can use a variety of energy substrates including FAs, glucose, lactate, ketones, and amino acids.[28] However, it is also regarded as a "pay as you go" energy consumer because it relies heavily on exogenous energy sources.[28] Although a rich body of work has delineated the metabolomic demands of hearts in physiological and diseased states,[29-31] understanding of the energy demands of DCD hearts is limited. In the OCS system, energy substrates for the heart are provided by a combination of postmortem donor blood and the priming and maintenance solution. However, it is unclear if this cocktail is optimally providing the necessary nutrients for the DCD heart.

Energy metabolism of the healthy heart depends mainly on the presence of FAs and glucose, while ketone bodies and amino acids have a secondary role.[32] In this study, we observed a striking decrease in FAs during perfusion for both human and porcine hearts. FAs are normally transported from the blood into the heart via lipoproteins or attached to albumin.[33] The marked decrease observed during perfusion from BL suggests that the heart quickly uses these substrates. Under aerobic conditions, FAs are the dominant fuel for a normal functioning heart. Many clinical and experimental studies suggest that during ischemic conditions, long-chain FAs may be harmful,[34] although less is known about the short- and medium-chain FAs identified in this study. In failing hearts, decreased transcription

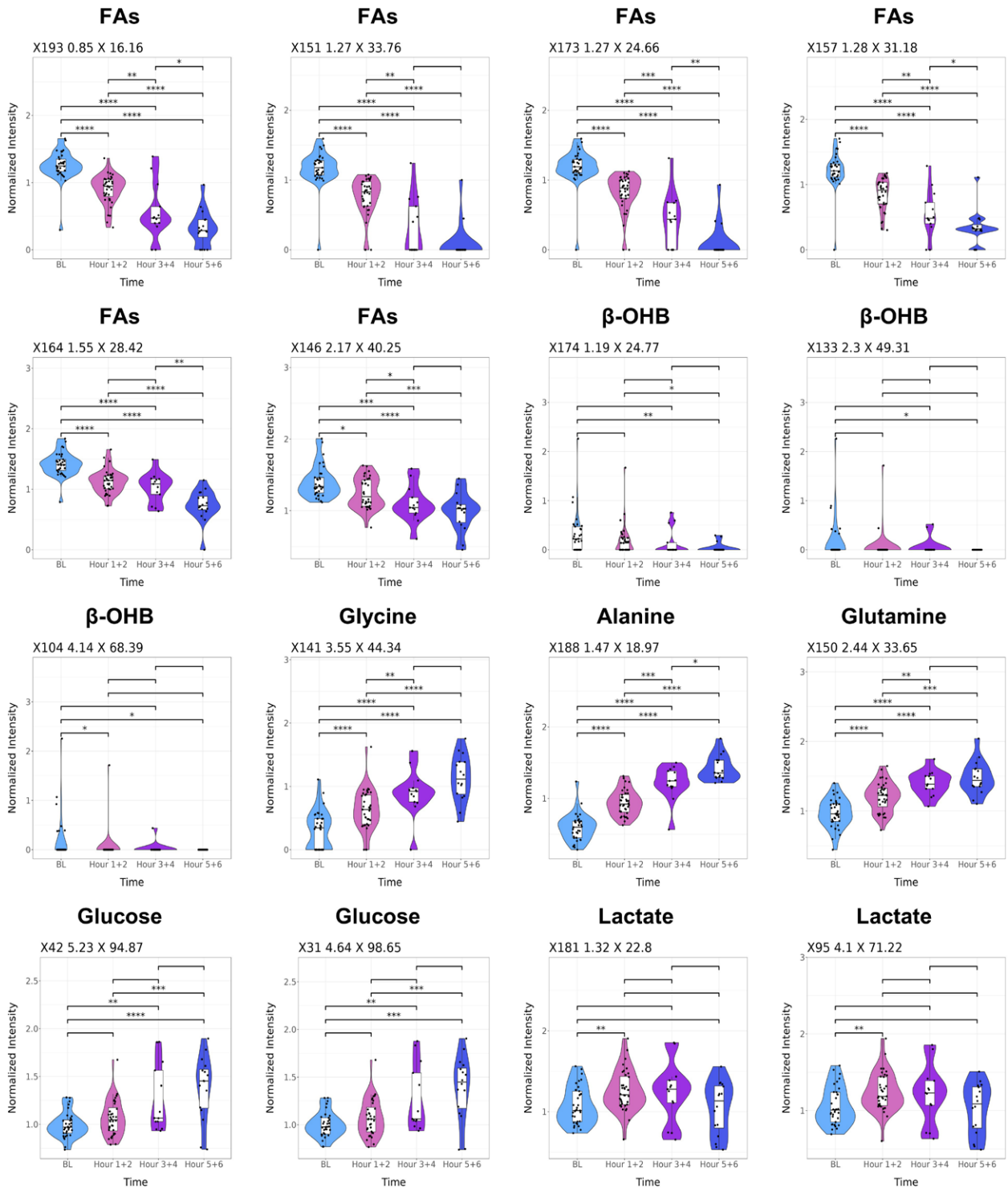

FIGURE 7. Choreography of energetic substrates during DCD MP. Violin plots depict changes in metabolite levels (shown as normalized intensity) for resonances of energy metabolites including FAs, β-OHB, the amino acids glycine, alanine, and glutamine and glucose and lactate during perfusion, from BL (light blue) through hours 1–2 (pink), 3–4 (purple), and 5–6 (dark blue) of perfusion. Annotations are listed above XIDs for each resonance. Significance values indicate Wilcoxon signed-rank test *P* value for all comparisons except 3–4 vs 5–6 h of perfusion, which are compared using Kruskal-Wallis test. **P* < 0.05; ***P* < 0.01; ****P* < 0.001; *****P* < 0.0001. Center values depict median; box plot range depicts first quartile (25%) through third quartile (75%). Whiskers depict 1.5 × (Q3–Q1) ± median and values outside whiskers indicate outliers. BL, baseline; DCD, donation after circulatory death; FA, fatty acid; MP, machine perfusion; β-OHB, β-hydroxybutyric acid, XID, feature number 1H x 13C ppm.

of enzymes for FA oxidation has been described, although contrasting results were observed for direct measurements of FAs.[17] An early study in rat models showed that animals exposed to high fat before DCD MP had significantly lower postischemic recovery suggesting that residual FAs exacerbate ischemia-reperfusion injury.[35] Furthermore, several

reports suggest that inhibitors of FA oxidation lessen postischemic cardiac dysfunction.[34] However, a separate study suggested that FA depletion led to exacerbated myocardial dysfunction in failing hearts and that both glucose and FA oxidation are critical.[36] Truby et al[18] also observed a decrease in nonesterified FAs during heart DCD MP. The marked decrease in FAs warrants further examination to determine what, if any, beneficial or harmful effects FAs have during DCD heart perfusion.

We also observed a decrease in the ketone β-OHB. In HF cardiac energy metabolism is dependent on ketone bodies produced in the liver, mainly β-OHB and acetone.[32,37,38] Acetone was not detected under our experimental conditions. Numerous studies have shown beneficial effects of administrating β-OHB to reduce pathological cardiac remodeling and improve cardiac function in small and large animal models of HF.[39,40] Moreover, infusion with β-OHB in patients with HF increases cardiac output by 40% without compromising myocardial energy efficiency.[41] A recent article by Seefeldt et al[42] also demonstrated its utility in a pig model of DCD transplant wherein in animals administered with β-OHB following circulatory death had improvements in cardiac measurements during perfusion and after transplant. Given the known cardioprotective role of β-OHB, future studies are aimed to explore its use as an additive during MP.

The amino acids alanine, glutamine, and glycine consistently increase from BL throughout perfusion for both human and porcine models. Truby et al[18] also observed an increase in several amino acids during MP, with alanine significantly correlated with troponin 1 and lactate. Alanine can be directly converted to pyruvate, while glycine can also be converted to pyruvate in a stepwise process of glycine to serine to cysteine to pyruvate. Pyruvate can feed the TCA cycle to generate energy through oxidative phosphorylation. Glutamine can also help drive oxidative phosphorylation by conversion first to glutamate then to the TCA substrate alpha-ketoglutarate. These results could suggest the heart is using amino acids as alternative scaffolds to support the TCA and oxidative phosphorylation. However, as the metabolomics measurements have been made in perfusate samples, we are not able to determine if the altered metabolites reflect cellular cardiac metabolism. Metabolites, especially amino acids, serve as signaling molecules.[43-51] Thus, the increased production of amino acids in the perfusate may need to be understood in this context. Future animal metabolomics studies exploring perfusate and myocardium are needed to decipher this interaction.

This study has several other limitations. Variability exists because of catecholamine surges during DCD, affecting cardiac function and lipid release.[52-54] Donor cause of death may also affect blood composition, although efforts were made to mitigate this through matched analysis. Furthermore, we were not able compare these results to DBD heart MP. However, there is a growing body of evidence in preclinical animal and human studies that suggest there are DCD and DBD specific patterns of substrate utilization.[7,55,56] We would also like to compare substrate utilization during MP in different organs and with different conditions/machines. Finally, more cohorts are needed for validation of the results.

Nonetheless, the results of this study support recent findings indicating a shift in energetic substrates during DCD heart MP. DCD heart transplantation has potential to increase organ availability. Understanding metabolic changes during MP postwarm ischemia is crucial for optimizing organ transplantation and widen adoption of this technology. This study provides a detailed examination of the time-dependent metabolomic profile of DCD MP hearts. Understanding these profiles is critical for rational nutrient supplementation design.

ACKNOWLEDGMENTS

The authors thank the Olaris team for thoughtful discussions and scientific contributions.

REFERENCES

1. Virani SS, Smith SC, Stone NJ, et al. Heart disease and stroke statistics—2020 update a report from the American Heart Association. *Circulation*. 2020;141:1121–1123.
2. Khush KK, Cherikh WS, Chambers DC, et al. The International Thoracic Organ Transplant Registry of the International Society for Heart and Lung Transplantation: thirty-fifth adult heart transplantation report—2018; focus theme: multiorgan transplantation. *J Heart Lung Transplant*. 2018;37:1155–1168.
3. Carvalho WDN, Maria GDSA, Gonçalves KC, et al. Comparison of quality of life between patients with advanced heart failure and heart transplant recipients. *Braz J Cardiovasc Surg*. 2021;36:623–628.
4. Arora S, Attawar S. Current status of cardiac transplantation in the 21st century. *Indian J Clin Cardiol*. 2022;3:94–102.
5. Koscik R, Ngai J. Donation after circulatory death: expanding heart transplants. *J Cardiothorac Vasc Anesth*. 2022;36:3867–3876.
6. Messer S, Cernic S, Page A, et al. A 5-year single-center early experience of heart transplantation from donation after circulatory-determined death donors. *J Heart Lung Transplant*. 2020;39:1463–1475.
7. Truby LK, Casalinova S, Patel CB, et al. Donation after circulatory death in heart transplantation: history, outcomes, clinical challenges, and opportunities to expand the donor pool. *J Card Fail*. 2022;28:1456–1463.
8. Schroder JN, Shah A, Pretorius V, et al. Expanding heart transplants from donors after circulatory death (DCD)—results of the first randomized controlled trial using the organ care system (OCS™) heart—(OCS DCD heart trial). *J Heart Lung Transplant*. 2022;41:S72.
9. Dhital K, Ludhani P, Scheuer S, et al. DCD donations and outcomes of heart transplantation: the Australian experience. *Indian J Thorac Cardiovasc Surg*. 2020;36:224–232.
10. Schroder JN, Patel CB, DeVore AD, et al. Transplantation outcomes with donor hearts after circulatory death. *N Engl J Med*. 2023;388:2121–2131.
11. Pagani FD. Heart transplantation using organs from donors following circulatory death: the journey continues. *J Am Coll Cardiol*. 2022;79:163–165.
12. Bertero E, Maack C. Metabolic remodelling in heart failure. *Nat Rev Cardiol*. 2018;15:457–470.
13. Shi X, Qiu H. New insights into energy substrate utilization and metabolic remodeling in cardiac physiological adaption. *Front Physiol*. 2022;13:831829.
14. Razeghi P, Young ME, Alcorn JL, et al. Metabolic gene expression in fetal and failing human heart. *Circulation*. 2001;104:2923–2931.
15. Neubauer S. The failing heart—an engine out of fuel. *N Engl J Med*. 2007;356:1140–1151.
16. Ng SM, Neubauer S, Rider OJ. Myocardial metabolism in heart failure. *Curr Heart Fail Rep*. 2023;20:63–75.
17. Karwi QG, Uddin GM, Ho KL, et al. Loss of metabolic flexibility in the failing heart. *Front Cardiovasc Med*. 2018;5:68.
18. Truby LK, Kwee LC, Bowles DE, et al. Metabolomic profiling during ex situ normothermic perfusion before heart transplantation defines patterns of substrate utilization and correlates with markers of allograft injury. *J Heart Lung Transplant*. 2024;43:716–726.
19. Roth HE, Powers R. Meta-analysis reveals both the promises and the challenges of clinical metabolomics. *Cancers (Basel)*. 2022;14:3992.

20. Lin Y, Caldwell GW, Li Y, et al. Inter-laboratory reproducibility of an untargeted metabolomics GC-MS assay for analysis of human plasma. *Sci Rep*. 2020;10:10918.
21. Zhang B, Powers R, O'Day EM. Evaluation of non-uniform sampling 2D1H–13C HSQC spectra for semi-quantitative metabolomics. *Metabolites*. 2020;10:203.
22. Connellan M, Dhital K. Donor heart procurement from the donation after circulatory death pathway. *Oper Tech Thorac Cardiovasc Surg*. 2017;22:58–67.
23. Khakimov B, Mobaraki N, Trimigno A, et al. Signature Mapping (SigMa): an efficient approach for processing complex human urine 1H NMR metabolomics data. *Anal Chim Acta*. 2020;1108:142–151.
24. Dieterle F, Ross A, Schlotterbeck G, et al. Probabilistic quotient normalization as robust method to account for dilution of complex biological mixtures. Application in1H NMR metabonomics. *Anal Chem*. 2006;78:4281–4290.
25. Delaglio F, Grzesiek S, Vuister GW, et al. NMRPipe: a multidimensional spectral processing system based on UNIX pipes. *J Biomol NMR*. 1995;6:277–293.
26. Ester M, Kriegel H-P, Sander J, et al. A density-based algorithm for discovering clusters in large spatial databases with noise. In: *Paper presented at:* Proceedings of the Second International Conference on Knowledge Discovery and Data Mining. Portland, OR; 1996.
27. Wickham H. *ggplot2: Elegant Graphics for Data Analysis*. Springer-Verlag; 2016.
28. Brooks GA. Role of the heart in lactate shuttling. *Front Nutr*. 2021;8:663560.
29. Lopaschuk GD, Karwi QG, Tian R, et al. Cardiac energy metabolism in heart failure. *Circ Res*. 2021;128:1487–1513.
30. Stanley WC, Recchia FA, Lopaschuk GD. Myocardial substrate metabolism in the normal and failing heart. *Physiol Rev*. 2005;85:1093–1129.
31. Doenst T, Nguyen TD, Abel ED. Cardiac metabolism in heart failure: implications beyond ATP production. *Circ Res*. 2013;113:709–724.
32. Papazafiropoulou A, Georgopoulos M, Katsilambros N. Ketone bodies and the heart. *Arch Med Sci Atheroscler Dis*. 2021;6:209–214.
33. van der Vusse GJ, van Bilsen M, Glatz JF. Cardiac fatty acid uptake and transport in health and disease. *Cardiovasc Res*. 2000;45:279–293.
34. Hendrickson SC, St Louis JD, Lowe JE, et al. Free fatty acid metabolism during myocardial ischemia and reperfusion. *Mol Cell Biochem*. 1997;166:85–94.
35. Niederberger P, Farine E, Arnold M, et al. High pre-ischemic fatty acid levels decrease cardiac recovery in an isolated rat heart model of donation after circulatory death. *Metabolism*. 2017;71:107–117.
36. Tuunanen H, Engblom E, Naum A, et al. Free fatty acid depletion acutely decreases cardiac work and efficiency in cardiomyopathic heart failure. *Circulation*. 2006;114:2130–2137.
37. Gjuladin-Hellon T, Davies IG, Penson P, et al. Effects of carbohydrate-restricted diets on low-density lipoprotein cholesterol levels in overweight and obese adults: a systematic review and meta-analysis. *Nutr Rev*. 2019;77:161–180.
38. Bhanpuri NH, Hallberg SJ, Williams PT, et al. Cardiovascular disease risk factor responses to a type 2 diabetes care model including nutritional ketosis induced by sustained carbohydrate restriction at 1 year: an open label, non-randomized, controlled study. *Cardiovasc Diabetol*. 2018;17:56.
39. Schugar RC, Moll AR, André d'Avignon D, et al. Cardiomyocyte-specific deficiency of ketone body metabolism promotes accelerated pathological remodeling. *Mol Metab*. 2014;3:754–769.
40. Horton JL, Davidson MT, Kurishima C, et al. The failing heart utilizes 3-hydroxybutyrate as a metabolic stress defense. *JCI Insight*. 2019;4:e124079.
41. Nielsen R, Møller N, Gormsen LC, et al. Cardiovascular effects of treatment with the ketone body 3-hydroxybutyrate in chronic heart failure patients. *Circulation*. 2019;139:2129–2141.
42. Seefeldt JM, Libai Y, Berg K, et al. Effects of ketone body 3-hydroxybutyrate on cardiac and mitochondrial function during donation after circulatory death heart transplantation. *Sci Rep*. 2024;14:757.
43. Cheng C, Kelsey S, Guo D. Glutamine-released ammonia acts as an unprecedented signaling molecule activating lipid production. *Genes Dis*. 2023;10:307–309.
44. Hensley CT, Wasti AT, DeBerardinis RJ. Glutamine and cancer: cell biology, physiology, and clinical opportunities. *J Clin Investig*. 2013;123:3678–3684.
45. Cruzat V, Rogero MM, Keane KN, et al. Glutamine: metabolism and immune function, supplementation and clinical translation. *Nutrients*. 2018;10:1564.
46. Giambelluca MS, Gende OA. Effect of glycine on the calcium signal of thrombin-stimulated platelets. *Blood Coagul Fibrinolysis*. 2007;18:303–308.
47. Schmidt RW, Thompson ML. Glycinergic signaling in the human nervous system: an overview of therapeutic drug targets and clinical effects. *Ment Health Clin*. 2016;6:266–276.
48. Aguayo-Cerón KA, Sánchez-Muñoz F, Gutierrez-Rojas RA, et al. Glycine: the smallest anti-inflammatory micronutrient. *Int J Mol Sci*. 2023;24:11236.
49. Felig P, Pozefsk T, Marlis E, et al. Alanine: key role in gluconeogenesis. *Science*. 1970;167:1003–1004.
50. Paudel S, Wu G, Wang X. Amino acids in cell signaling: regulation and function. *Adv Exp Med Biol*. 2021;1332:17–33.
51. Cunningham GA, McClenaghan NH, Flatt PR, et al. L-alanine induces changes in metabolic and signal transduction gene expression in a clonal rat pancreatic β-cell line and protects from pro-inflammatory cytokine-induced apoptosis. *Clin Sci (Lond)*. 2005;109:447–455.
52. Iyer A, Chew HC, Gao L, et al. Pathophysiological trends during withdrawal of life support: implications for organ donation after circulatory death. *Transplantation*. 2016;100:2621–2629.
53. Arnold M, Méndez-Carmona N, Wyss RK, et al. Comparison of experimental rat models in donation after circulatory death (DCD): in-situ vs. ex-situ ischemia. *Front Cardiovasc Med*. 2021;7:596883.
54. White CW, Lillico R, Sandha J, et al. Physiologic changes in the heart following cessation of mechanical ventilation in a porcine model of donation after circulatory death: implications for cardiac transplantation. *Am J Transplant*. 2016;16:783–793.
55. Cirillo A, Vandermeulen M, Erpicum P, et al. Untargeted NMR-based metabolomics analysis of kidney allograft perfusates identifies a signature of delayed graft function. *Metabolomics*. 2024;20:39.
56. Hautbergue T, Laverdure F, Van SD, et al. Metabolomic profiling of cardiac allografts after controlled circulatory death. *J Heart Lung Transplant*. 2023;42:870–879.